CrossMark

Vanadium(IV/V) complexes of Triapine and related thiosemicarbazones: Synthesis, solution equilibrium and bioactivity

Christian R. Kowol [a,b,*], Nóra V. Nagy [c], Tamás Jakusch [d], Alexander Roller [a], Petra Heffeter [b,e], Bernhard K. Keppler [a,b], Éva A. Enyedy [d,*]

[a] University of Vienna, Institute of Inorganic Chemistry, Währinger Strasse 42, A-1090 Vienna, Austria
[b] Research Platform "Translational Cancer Therapy Research" University of Vienna, Waehringer Strasse 42, A-1090 Vienna, Austria
[c] Institute of Organic Chemistry, Research Centre for Natural Sciences, Hungarian Academy of Sciences, Magyar Tudósok körútja 2, H-1117 Budapest, Hungary
[d] Department of Inorganic and Analytical Chemistry, University of Szeged, H-6720 Szeged, Hungary
[e] Institute of Cancer Research and Comprehensive Cancer Center, Medical University of Vienna, Borschkegasse 8a, A-1090 Vienna, Austria

ARTICLE INFO

ABSTRACT

The stoichiometry and thermodynamic stability of vanadium(IV/V) complexes of Triapine and two related α(N)-heterocyclic thiosemicarbazones (TSCs) with potential antitumor activity have been determined by pH-potentiometry, EPR and ^{51}V NMR spectroscopy in 30% (w/w) dimethyl sulfoxide/water solvent mixtures. In all cases, mono-ligand complexes in different protonation states were identified. Dimethylation of the terminal amino group resulted in the formation of vanadium(IV/V) complexes with considerably higher stability. Three of the most stable complexes were also synthesized in solid state and comprehensively characterized. The biological evaluation of the synthesized vanadium complexes in comparison to the metal-free ligands in different human cancer cell lines revealed only minimal influence of the metal ion. Thus, in addition the coordination ability of salicylaldehyde thiosemicarbazone (STSC) to vanadium(IV/V) ions was investigated. The exchange of the pyridine nitrogen of the α(N)-heterocyclic TSCs to a phenolate oxygen in STSC significantly increased the stability of the complexes in solution. Finally, this also resulted in increased cytotoxicity activity of a vanadium(V) complex of STSC compared to the metal-free ligand.

© 2015 Elsevier Inc. All rights reserved.
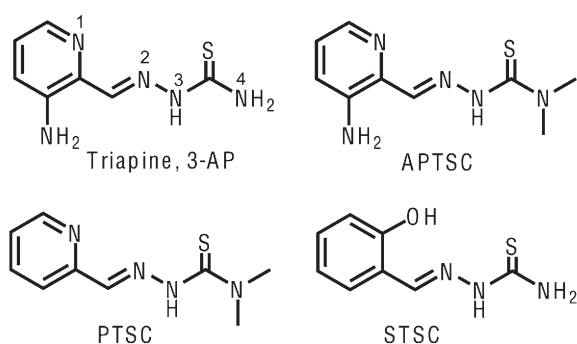
1. Introduction

Thiosemicarbazones (TSCs) are Schiff bases obtained by condensation of an aldehyde or a ketone with a thiosemicarbazide and represent an important class of (N,S) donor ligands [1]. TSCs and their metal complexes are extensively investigated as they exhibit a wide range of pharmacologically interesting properties like anticancer, antibacterial, antiparasitic, and antiviral effects [2]. Especially α(N)-heterocyclic TSCs exert significant antitumor activity *in vitro* and *in vivo* [2,3]. Triapine (3-aminopyridine-2-carbaldehyde thiosemicarbazone, 3-AP, Chart 1) is the most prominent representative among the α(N)-pyridyl TSCs since it has already been tested in many phase I and II clinical trials [4]. The proposed mechanism of action of Triapine is based on its ability to inhibit the iron-dependent enzyme ribonucleotide reductase, the rate-determining enzyme in the supply of deoxyribonucleotides for DNA synthesis and repair [3,5]. It has been assumed that the formation of an intracellular iron complex of Triapine plays a crucial role in the mechanism of enzyme inhibition [6]. In this complex, Triapine acts as

tridentate ligand and coordinates *via* an (N_{pyr},N,S$^-$) donor set, wherein the hydrazinic-N moiety is deprotonated [3]. In general, this arrangement of the donor atoms for α(N)-pyridyl TSCs is also suitable for the binding of other transition metal ions, *e.g.* Cu(II), Zn(II), Ru(III), Pt(II), and Pd(II), which can result in complexes with even higher cytotoxicity than that of the metal-free ligands [2]. In our previous works we pointed out that dimethylation of the terminal nitrogen strongly enhances the cytotoxicity of α(N)-pyridyl TSCs, especially in the absence of any NH$_2$ group in the molecule [7]. In addition, terminal dimethylation results in a strong increase of the solution stability of the Fe(II/III), Cu(II), Zn(II), and Ga(III) complexes [7–9]. The best-known terminally dimethylated bis-pyridyl TSC is di-2-pyridylketone-4,4-dimethyl-3-thiosemicarbazone (Dp44mT), which demonstrated very potent anticancer activity *in vivo* using human xenografts in nude mice [10,11] and was reported to overcome multidrug-resistance in cancer cells [12].

In addition, to the effects of the free ligands, also a wide range of metal complexes of tridentate TSCs with remarkable biological effect has been reported in the literature including copper [13–15], platinum [16], or vanadium compounds [2,17,18]. With regard to vanadium, complexes of α(N)-pyridyl TSCs formed with oxovanadium(IV) and dioxovanadium(V) were found to exert antibacterial, antifungal as well as antiamoebic activity [17–20]. In addition, insulin-enhancing
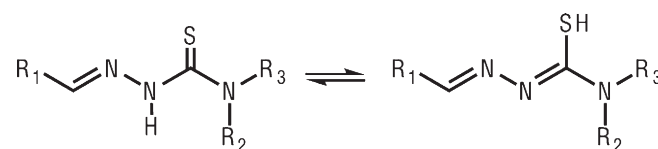
* Corresponding authors.
  E-mail addresses: christian.kowol@univie.ac.at (C.R. Kowol), enyedy@chem.u-szeged.hu (É.A. Enyedy).

Chart 1. Ligands used in this study: Triapine (3-AP) = 3-aminopyridine-2-carboxaldehyde thiosemicarbazone; APTSC = 3-aminopyridine-2-carboxaldehyde N,N-dimethylthiosemicarbazone; PTSC = pyridine-2-carboxaldehyde N,N-dimethylthiosemicarbazone; STSC = salicylaldehyde thiosemicarbazone.

Chart 2. Tautomerism of thiosemicarbazones.

salicylaldehyde thiosemicarbazone (STSC, Chart 1) complexes with an (O⁻,N,S⁻) donor set.

2. Results and discussion

2.1. Solution chemistry of vanadium(IV/V) complexes of Triapine, APTSC, and PTSC

2.1.1. pK_a values and lipophilicity of the ligands

The proton dissociation constants (pK_a) of Triapine, APTSC and PTSC (Table 1) in a 30% (w/w) DMSO/H$_2$O solvent mixture were already determined in our previous work by pH-potentiometric, UV–vis, and ^{1}H NMR titrations [8]. In accordance with these data, the repetitive measurements in this study provided similar values. Noteworthy, the presence of DMSO was required due to the limited water solubility of the ligands as well as their respective vanadium complexes. The obtained pK_1 can be attributed to the proton dissociation of the pyridinium unit and pK_2 values to the deprotonation of the hydrazinic NH group of the thiosemicarbazide moiety. In the latter proton dissociation step, the resulting negative charge is mainly localized on the S atom *via* the thione–thiol tautomeric equilibrium (Chart 2) [8]. Based on the pK_a values, it can be concluded that all three α-pyridyl TSCs are present in their neutral HL form at pH 7.4.

In order to characterize the lipophilic character of the ligands, distribution coefficients of APTSC and PTSC were determined by the traditional shake flask method at pH 7.4 ($\log D_{7.4}$ values in Table 1), which represent the actual partitioning between *n*-octanol and water. As expected, the methyl groups on the terminal nitrogen of the α-pyridyl TSCs increase the $\log D_{7.4}$ value compared to that of the reference compound Triapine [25].

2.1.2. Complex formation equilibria of vanadium(IV) with Triapine, APTSC, and PTSC

The complex formation processes of Triapine, APTSC, and PTSC with V(IV)O were studied by the combined approach of pH-potentiometry, UV–vis spectrophotometry, and EPR spectroscopy in a 30% (w/w) DMSO/H$_2$O solvent mixture under anaerobic conditions. The stoichiometries of

properties of some V(V)O$_2$–TSC complexes have been reported [21]. However, the antitumor properties of α(N)-pyridyl TSC vanadium complexes have, to the best of our knowledge, not been investigated so far. Moreover, despite the fact that a relatively large number of vanadium(IV/V) complexes of TSCs has been synthesized and characterized in the solid state or in solution with organic solvents [19–24], almost no information is available on their complex formation processes and thermodynamic stability in aqueous solution. Notwithstanding, the knowledge of the speciation and the most feasible chemical forms of a biologically active metal complex in aqueous solution, especially at physiological pH, can help to understand the mechanism of action and might be useful for the design of more effective and selective chemotherapeutics. Thus, the main aims of the present work were to perform a detailed solution equilibrium study on the vanadium(IV/V) complexes of Triapine and two terminally dimethylated derivatives (Chart 1, 3-aminopyridine-2-carboxaldehyde N,N-dimethylthiosemicarbazone (APTSC) and pyridine-2-carboxaldehyde N,N-dimethylthiosemicarbazone (PTSC)), and to screen their cytotoxicity against human cancer cell lines. Therefore, various methods such as pH-potentiometry, UV–vis spectrophotometry as well as electron paramagnetic resonance (EPR) and ^{51}V NMR spectroscopy were used to investigate the stoichiometry and stability of the complexes in solution. Additionally, several vanadium complexes were synthesized and subsequently characterized by means of ^{1}H, ^{13}C, and ^{51}V NMR spectroscopy as well as X-ray diffraction studies. Finally, the obtained solution speciation data of the vanadium(IV/V) complexes formed with α(N)-pyridyl TSCs were compared to that of

Table 1
Proton dissociation constants (pK_a) and $\log D_{7.4}$ values of the studied TSC ligands as well as overall ($\log\beta$), stepwise and conditional stability constants for their V(IV)O complexes {T = 25.0 °C, I = 0.10 M (KCl) in 30% (w/w) DMSO/H$_2$O}.[a]

	Triapine	APTSC	PTSC	STSC
pK_1	3.92[b]	4.31[b]	3.38[b]	8.89[c]
pK_2	10.78[b]	10.29[b]	10.54[b]	12.59[c]
$\log D_{7.4}$	+0.85[c]	+1.30(8)	+1.11(15)	+1.74[c]
$\log\beta$ [V(IV)O(LH)]	–	–	–	20.55(2)
$\log\beta$ [V(IV)O(L)]	8.50(8)	10.30(4)	10.83(2)	16.67(1)
$\log\beta$ [V(IV)O(L)H$_{-1}$]	3.21(9)	4.14(12)	4.74(5)	9.79(1)
pK [V(IV)O(L)]	5.29	6.16	6.09	6.88
Fitting parameter (mL)	4.90×10^{-3}	3.25×10^{-3}	2.90×10^{-3}	3.08×10^{-3}
$\log K'$ [V(IV)O(L)][d]	7.23	8.67	9.02	10.61
Predominant complex[e]	([V(IV)O$_2$(OH)$_5$])	[V(IV)O(LH$_{-1}$)]	[V(IV)O(LH$_{-1}$)]	[V(IV)O(LH$_{-1}$)]

[a] Uncertainties (SD) of the last digits are shown in parentheses determined for the TSCs studied in the present work. Charges of the metal complexes are omitted for clarity.
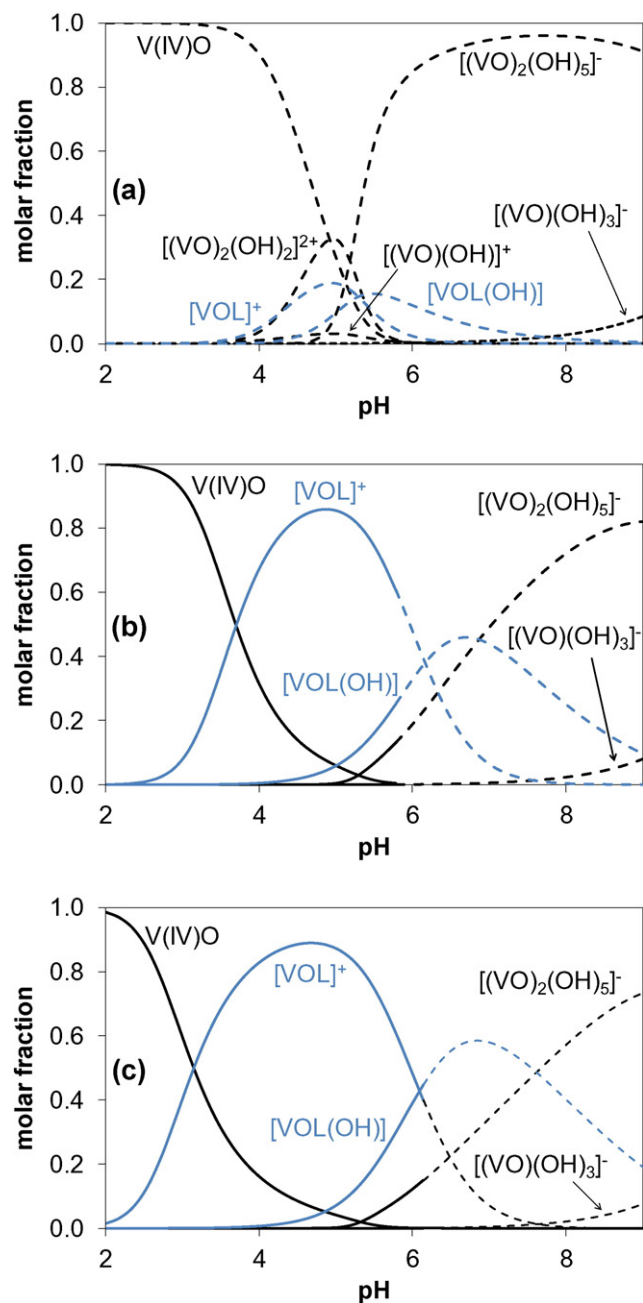[b] Taken from [8].
[c] Taken from [25].
[d] Conditional stability constants at pH = 7.4; $K' = \beta$ [V(IV)O(L)] $\times$ (1 + β [V(IV)O(L)H$_{-1}$] / [H$^+$] / β [V(IV)O(L)]) / (1 + [H$^+$] $\times \beta_{HL}$ + [H$^+$]$^2 \times \beta_{H2L}$).
[e] At pH = 7.4; $c_{V(IV)O}$ = 1.0 mM; V(IV)O:L = 1:1.

the oxovanadium(IV) complexes and the overall stability constants calculated on the basis of the pH-potentiometric titrations are listed in Table 1. These studies revealed the formation of mono-ligand complexes such as $[V(IV)O(L)]^+$ and $[V(IV)O(L)H_{-1}]$. Although, other bivalent metal ions (e.g. Zn(II) and Fe(II)) form $[M(LH)]^{2+}$ species as well [8], stability constants for this kind of V(IV)O complexes could not be calculated with appropriate accuracy. Complexation of Triapine with V(IV)O starts only at pH > 4 and the ligand is not able to protect the metal ion against the hydrolysis at a metal-to-ligand ratio of 1:1 at pH > 6 in the 1 mM concentration range resulting in precipitation. Notably, a maximum of 20% of V(IV)O is bound to Triapine (at pH ~ 5 under this condition) representing a quite weak metal-binding ability of this ligand (Fig. 1a). On the contrary, complex formation
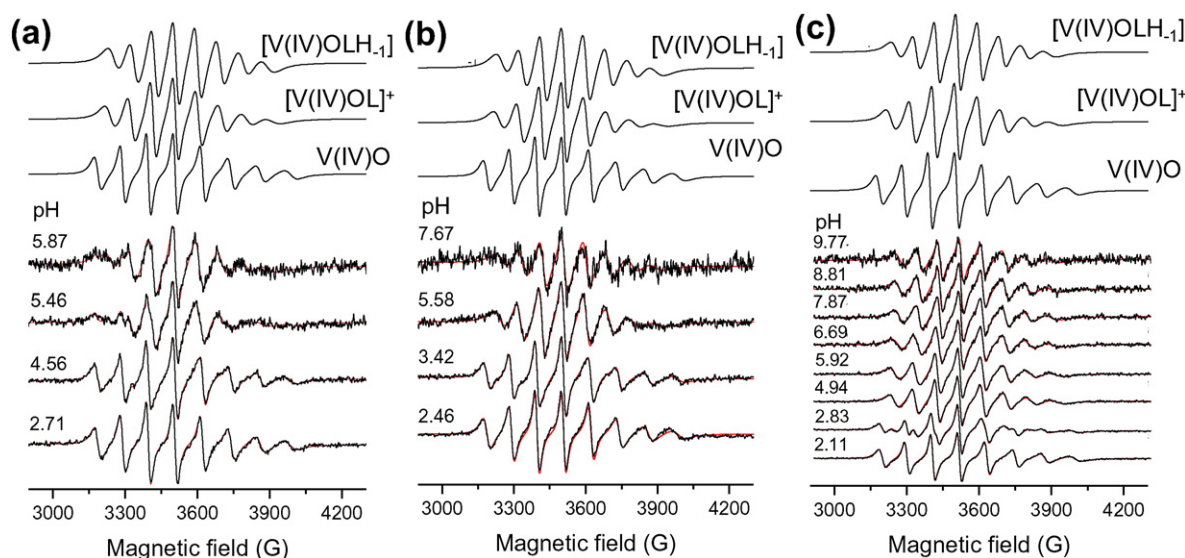
processes with the terminally dimethylated ligands (PTSC and APTSC) start at lower pH values (pH ~ 2–2.5) indicating species of higher stability. In addition, the bound fraction of oxovanadium(IV) exceeds 90% at pH ~ 5.2 and 4.5 in the V(IV)O–APTSC and PTSC systems, respectively (Fig. 1b and c). Complex formation in the V(IV)O–PTSC system was also monitored by UV–vis spectrophotometric titrations. Instead of the rather weak d–d transition bands of the complexes, the pH-dependence of the overlapping charge-transfer (CT) and ligand bands was followed. Differences between the absorbance values recorded in the presence and in the absence of the V(IV)O ions undoubtedly reveal the pH ranges of the complex formation followed by dissociation. This corresponds well to the expectations based on the concentration distribution curves calculated with the aid of the stability constants (Fig. S1).

In order to elucidate the actual coordination modes in solution and confirm the speciation model obtained by pH-potentiometry, EPR spectra were recorded at various pH values at room temperature (Fig. 2). In case of the V(IV)O–PTSC system, spectra could be recorded up to pH 9.8 using individual samples. In contrast, when titrations were performed with Triapine and APTSC, oxidation took place resulting in the continuous loss of the EPR signal at higher pH values, although the measurements were done under an argon atmosphere (but not under strictly anaerobic conditions). It is noteworthy, that the hydrolysis of the metal ion can strongly increase the sensitivity to oxidation. The two-dimensional simulation of the solution EPR spectra resulted in the individual isotropic EPR spectra (Fig. 2) and the isotropic EPR parameters of V(IV)O and the complexes $[V(IV)O(L)]^+$ and $[V(IV)O(L)H_{-1}]$ (Table 2). There was no indication for the formation of EPR-active dinuclear or bis-ligand complexes. Similar g_0 and A_0 values were obtained for all $[V(IV)O(L)]^+$ complexes of the different α-pyridyl TSCs, in which the tridentate coordination of the ligands via the (N_{pyr}, N^2, S^-) donor set is the most probable and where the ligand possesses a deprotonated hydrazinic moiety. In comparison, formation of isomers and somewhat higher A_0 parameters (94.7×10^{-4} cm^{-1} and 101×10^{-4} cm^{-1}) were reported for chlorido V(IV)O-thiosemicarbazone complexes in a non-aqueous solvent [26]. Complexes $[V(IV)O(L)H_{-1}]$ have higher g_0 values and lower A_0 values compared to those of $[V(IV)O(L)]^+$ indicating an increased ligand field due to the deprotonation of the coordinated water molecule. As a consequence, $[V(IV)O(L)H_{-1}]$ complexes are considered as mixed hydroxido species $[V(IV)O(L)(OH)]$. Using the empirical additivity relationship [27,28], the average A_0 value of the contribution of a thiolate, two aromatic nitrogen atoms (no data for imine-N) and a water molecule is 87.0×10^{-4} cm^{-1} and for the mixed hydroxido species 80.6×10^{-4} cm^{-1}. All estimations are in good agreement with the measured data in Table 2.

In the case of the V(IV)O–PTSC system, EPR spectra were also recorded on frozen samples at 77 K. The calculated anisotropic EPR parameters (Table 3) and the spectra simulation for the $[V(IV)O(L)]^+$ and $[V(IV)O(L)H_{-1}]$ species (Fig. 3) permitted the conclusion that most probably two kinds of isomers with a molar ratio of ~1:6 are formed under these conditions. The isotropic EPR parameters of the major isomers (1) calculated by averaging the anisotropic values ($g_{0,calc}$ and $A_{0,calc}$ in Table 3) are similar to those of the data measured at room temperature showing that the structure of the complexes $[V(IV)O(L)]^+$ and $[V(IV)O(L)H_{-1}]$ did not change during freezing. On the other hand, the minor isomers (2) have fairly different anisotropic EPR parameters, which can be possibly explained by the octahedral "trans" (H$_2$O: axial, PTSC: equatorial, equatorial, equatorial, H$_2$O/OH$^-$ equatorial) penta-coordinated square pyramidal or octahedral "trans" – octahedral "cis" (H$_2$O: equatorial, PTSC: equatorial, axial, equatorial, H$_2$O/OH$^-$ equatorial) – isomerism [29]. This is quite frequent in the case of V(IV)O species and was also observed for other V(IV)O–TSC complexes [24,26]. In the protonation state of VO(IV)L the octahedral "trans", while in the case of complex $[V(IV)OL(OH)]$ the penta-coordinated/octahedral "cis" forms are the most stable species.

Direct comparison of stability constants and concentration distribution curves calculated for the V(IV)O complexes formed with the

Fig. 1. Representative concentration distribution diagrams for V(IV)O complexes formed in the V(IV)O — Triapine (a), APTSC (b) and PTSC (c) systems plotted against the pH calculated on the basis of the pH-potentiometric results. {V(IV)O:L = 1:1; c_{ligand} = 2.0 mM; T = 25.0 °C, I = 0.10 M (KCl) in 30% (w/w) DMSO/H$_2$O}. Dashed lines indicate the pH range where significant amounts of hydrolyzed V(IV)O species are formed.

Fig. 2. Experimental (black) and simulated (red) isotropic EPR spectra recorded for the V(IV)O — Triapine (a), APTSC (b) and PTSC (c) systems together with the calculated component EPR spectra of the various species. Spectral intensities have been normalized for better comparison. {c_{ligand} = 1.0 mM; V(IV)O:L = 1:2, 1:2 and 1:4 for APTSC, PTSC and Triapine, respectively; T = 25.0 °C, I = 0.10 M (KCl) in 30% (w/w) DMSO/H$_2$O}.

α-pyridyl TSCs (Table 1, Fig. 1) shows that Triapine is hardly able to form stable complexes with V(IV)O even at mM concentrations. In contrast, the complex stability of terminally dimethylated TSCs is distinctly increased. This is in good agreement with previous studies from our group on other metal ions [8,9].

2.1.3. Complex formation equilibria of vanadium(V) with Triapine, APTSC, and PTSC

As a next step, the V(V)-binding abilities of Triapine, APTSC, and PTSC were studied by ^{51}V NMR spectroscopy. This method provides an excellent possibility to distinguish between the free V(V) species (in monomeric or different oligomeric forms) and V(V) complexes due to the slow ligand-exchange process with respect to the NMR time scale. Therefore, signals of bound and free metal ions can be seen separately (as an example, PTSC is shown in Fig. 4a). However, species with the same metal-to-ligand ratio in different protonation states represent fast exchange processes. Thus, their signals are only shifted upon the (de)protonation processes. First of all, complex formation was followed at pH 7.4 in the 1.0 mM concentration range. No bound V(V) fractions were found in the case of Triapine as a consequence of the quite low vanadate affinity of this ligand. Accordingly, further measurements were only performed for APTSC and PTSC.

^{51}V NMR spectra were recorded in the pH range 11.2–~1.6 by the addition of strong acid to the samples, although an irreversible process was observed at pH < 5 and the intensities of the peaks were strongly

Table 2
Isotropic EPR parameters obtained for the V(IV)O–TSC complexes calculated from the two-dimensional simulation of EPR spectra {T = 25.0 °C, I = 0.10 M (KCl) in 30% (w/w) DMSO/H$_2$O}.[a]

Ligand	Species	g_0	$A_0/\times 10^{-4}$ cm^{-1}	α/G	β/G	γ/G
–	V(IV)O^{2+}	1.9616(2)	104.5(2)	18.7(1)	3.5(1)	1.8(1)
Triapine	[V(IV)O(L)]$^+$	1.9703(8)	87.8(8)	23(2)	5(1)	2.8(3)
Triapine	[V(IV)O(L)H$_{-1}$]	1.972(2)	82.9(4)	26(7)	3(2)	3(1)
APTSC	[V(IV)O(L)]$^+$	1.9709(9)	87.4(1)	23(7)	5(2)	3.3(1)
APTSC	[V(IV)O(L)H$_{-1}$]	1.971(2)	79.1(3)	26(7)	3(2)	3(1)
PTSC	[V(IV)O(L)]$^+$	1.9702(2)	88.7(6)	19(3)	4(1)	2.3(5)
PTSC	[V(IV)O(L)H$_{-1}$]	1.9711(4)	83.1(6)	19(7)	3(2)	2(1)
STSC	[V(IV)O(L)]	1.9717(7)	87.6(7)	21(1)	3(1)	2.0(3)

[a] Uncertainties (SD) of the last digits are shown in parentheses determined in the present work.

diminished. Most probably V(V) is able to oxidize APTSC and PTSC in this pH range with simultaneous formation of paramagnetic V(VI)O. Interestingly, a similar redox reaction was already described for Fe(III) complexes of α(N)-pyridyl TSCs, however only at pH > 10 [9,30]. Solely peaks of the non-bound V(V) species could be observed at pH > ~10, in the case of PTSC (Fig. 4a) and APTSC, mainly in a form of HVO$_4^{2-}$. Formation of [V(V)O$_2$(L)] was further investigated with decreasing pH and the position of its signal in the NMR spectra did not change down to pH ~ 5. In this complex, most probably coordination of two oxo groups and the deprotonated ligand through the (N$_{pyr}$,N^2,S$^-$) donor atoms results in a distorted square-pyramidal geometry (Chart 3). This coordination mode was also confirmed by X-ray crystal structure analysis of solid V(V)–PTSC and V(V)–APTSC complexes (Section 2.2). Subsequently, the distribution of V(V) between bound and unbound fractions at a 1:1 metal-to-ligand ratio was calculated on the basis of the integrated area of the peaks for the V(V)–PTSC and APTSC systems (Fig. 4b). From these values, stability constants were computed for the formation of [V(V)O$_2$(L)] complexes (see Table 4 for the equilibrium processes and constants). The bound V(V) fraction is slightly higher for PTSC compared to APTSC (91% vs. 82%), and the bound metal ion fraction is higher in the case of the V(V)-containing systems compared to V(IV)O representing a somewhat higher stability of the V(V) complexes.

2.2. Synthesis and characterization of vanadium(IV/V) complexes of PTSC and APTSC

As a result of the solution equilibrium studies, it was concluded that Triapine is not an efficient chelator for vanadium(IV/V) ions. Therefore, we prepared only the vanadium complexes of the terminally dimethylated ligands (PTSC and APTSC) for further biological studies. The two metal-free ligands APTSC and PTSC were synthesized according to literature [7,31]. The V(V)O$_2$-containing complexes were synthesized in methanol in 1:2 molar ratio using the appropriate TSC ligand (HL) and the vanadium(V) precursor V$_2$O$_4$(acac)$_2$ (where acac = acetylacetonate) [32]. This resulted in formation of the orange and red [V(V)O$_2$(L)] complexes of PTSC (**1a**) and APTSC (**1b**), respectively, in good yields (Chart 3). The green oxovanadium(IV) complex [V(IV)O(L)(acac)] of PTSC (**2a**) (Chart 3) was synthesized in ethanol in 78% yield using VO(acac)$_2$ and the ligand in a 1:1 molar ratio.

The ^{1}H NMR spectrum of the V(V)O$_2$ complexes confirmed deprotonation of the TSC ligands by the absence of the NH proton signal of

Table 3
Anisotropic EPR parameters obtained for the V(IV)O–PTSC complexes {$T = 77$ K, $I = 0.10$ M (KCl) in 30% (w/w) DMSO/H$_2$O}.[a]

	$g_{\parallel}$	$g_{\perp}$	$A_{\parallel}/\times 10^{-4}$ cm^{-1}	$A_{\perp}/\times 10^{-4}$ cm^{-1}	$g_{o,calc}$[b]	$A_{o,calc}$[c]$/\times 10^{-4}$ cm^{-1}
V(IV)O^{2+}	1.9325	1.9743	179.7	67.5	1.9604	104.9
[V(IV)O(L)]$^+$ (1)	1.9525	1.9801	158.2	54.4	1.9709	89.0
[V(IV)O(L)]$^+$ (2)	1.9470	1.9788	164.5	59.6	1.9672	94.6
[V(IV)O(L)H$_{-1}$] (1)	1.9546	1.9801	153.6	50.5	1.9716	84.9
[V(IV)O(L)H$_{-1}$] (2)	1.9683	1.9823	143.6	45.6	1.9776	78.3

[a] The experimental error was ± 0.001 for $g_{\parallel}$, ± 0.0005 for $g_{\perp}$, $\pm 0.5 \times 10^{-4}$ cm^{-1} for $A_{\parallel}$ and $\pm 0.2 \times 10^{-4}$ cm^{-1} for $A_{\perp}$.
[b] $g_{0,calc} = (g_{\parallel} + 2 g_{\perp}) / 3$.
[c] $A_{0,calc} = (A_{\parallel} + 2A_{\perp}) / 3$.

the thiosemicarbazide moiety. Furthermore, in contrast to the metal-free PTSC, which shows two isomeric forms [33] in DMSO-d_6, the V(V)O$_2$ complexes possess only one set of signals in the ^{1}H NMR spectra. This can be explained by stabilization of the ligand configuration upon coordination to the metal center. The ^{51}V NMR shifts of **1a** at -427.5 and **1b** at -430.0 ppm measured in DMSO-d_6 were in the expected range of this type of vanadium complexes [21].

Single crystals of X-ray diffraction quality of **1a** were obtained after several days directly from the mother liquor. In contrast, crystals of **2a** were produced by slow diffusion of ether into a solution of the complex in CH$_2$Cl$_2$ under argon atmosphere. Crystal data, data collection parameters, and structure refinement details are given in Table S1. The results of the X-ray diffraction studies are shown in Fig. 5 and selected bond distances and angles are summarized in Table 5 for **1a** and **2a** in comparison to the PTSC ligand [7]. For the vanadium(V) complex **1a** (Fig. 5), the coordination polyhedron around the metal ion is intermediate between square-pyramidal and trigonal-bipyramidal with $\tau = 0.37$ ($\tau = 1$ for an ideal trigonal bipyramid, $\tau = 0$ for an ideal square pyramid) [34]. The vanadium(V) is coordinated by one tridentate deprotonated PTSC ligand (L$^-$) *via* the pyridine nitrogen atom as well as the nitrogen and sulfur donors of the thiosemicarbazide moiety and two oxido ligands with bond length in the expected range for such type of complexes [21,24].

In contrast, in the oxovanadium(IV) complex **2a**, the coordination polyhedron approaches an octahedron, where one tridentate PTSC, a bidentate acac, and an oxido ligand is coordinated to the metal center (Fig. 5). Comparably to complex **1a**, the ligand is deprotonated (L$^-$).
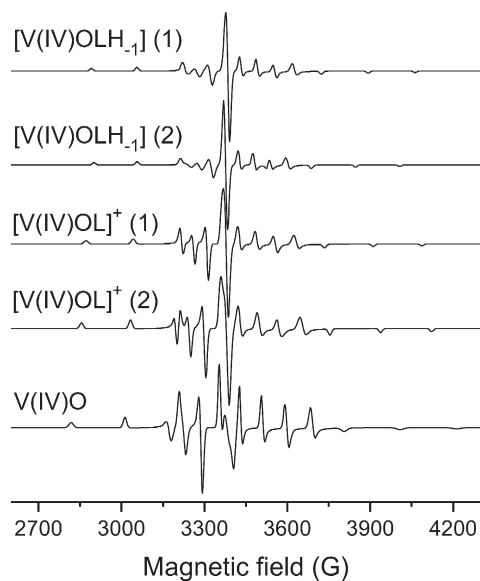
Of note is the difference in the bond length from vanadium(IV) to the acac oxygen atoms with V–O1 at 1.984 Å and V–O2 at 2.155 Å. The enlongated bond length of V–O2 can be explained by the *trans* influence of the oxido ligand and is in agreement with a similar structure with 2-acetylpyridine-4-phenylthiosemicarbazone [35]. In crystal structures of both, **1a** and **2a**, deprotonation of the PTSC ligand is accompanied with a distinct elongation of the C7–S bond (**1a**: 1.737 Å; **2a**: 1.751 Å) compared to the metal-free ligand at 1.686 Å indicating an increased single-bond character [7]. In addition, the C7–N3 bond decreases from 1.373 Å to 1.325 Å in **1a** and 1.334 Å in **2a**, respectively.

2.3. Cytotoxicity of complexes **1a**, **1b**, and **2a**

As a next step, the cytotoxicity of the novel synthesized compounds (IC$_{50}$ values in nM) of **1a**, **1b**, and **2a** in comparison to their metal-free ligands was measured in three human cancer cell lines (colon carcinoma SW480, ovarian carcinoma A2780, and epidermal carcinoma-derived KB-3-1 cells). Table 6 shows the IC$_{50}$ values for the compounds after 72 h incubation measured by the 3-(4,5-dimethyl-2-thiazolyl)-2,5-diphenyl-2H-tetrazolium bromide (MTT) assay.

In general, A2780 cells were found to be the most sensitive of the investigated cell lines, whereas SW480 and KB-3-1 cells were less affected by the compounds. In accordance to the literature, PTSC had IC$_{50}$ values in the (low) nanomolar range, whereas, APTSC was active at low μM concentrations comparable to Triapine [7]. Interestingly, the sensitivity profile of SW480 cells was strongly different from KB-3-1 and A2780. These two cell models were very sensitive towards PTSC and its complexes, while in SW480 cells a distinctly reduced activity was observed. In contrast, APTSC and its vanadium complex showed quite similar activity in all three cell lines. This probably originates from differences in the mode of action, which were observed for PTSC compared to APTSC [36]. Despite these differences originating from the ligand properties, the impact of vanadium complexation was rather weak. Thus, only in KB-3-1 cells a non-significant tendency for increased activity of **1a** and **2a** in comparison to the respective free ligand was observed. In contrast, **1b** was slightly less active than APTSC in all tested cell lines. This lack of impact can most probably be explained by the release of the ligands due to the low solution stability of these vanadium complexes already in the low micro- to nanomolar concentration range.
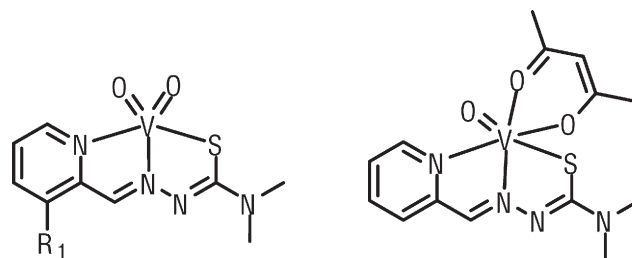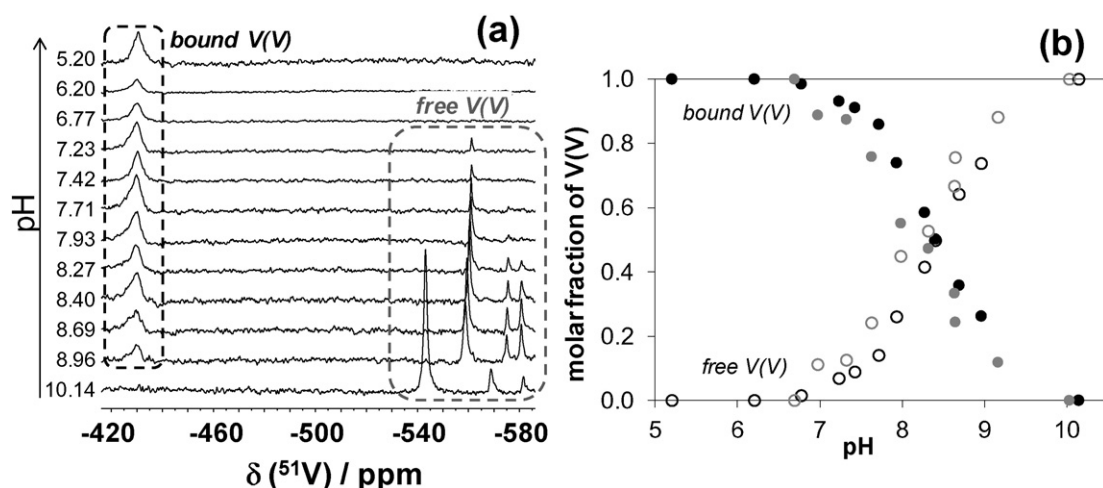

Fig. 3. Calculated component anisotropic EPR spectra of V(IV)O and various isomeric species formed in the V(IV)O–PTSC system. {$T = 77$ K, $I = 0.10$ M (KCl) in 30% (w/w) DMSO/H$_2$O}.

Chart 3. Structures of the synthesized complexes **1a** (R$_1$ = H), **1b** (R$_1$ = NH$_2$) and **2a**.

Fig. 4. ^{51}V NMR spectra recorded for the V(V)–PTSC system at various pH values (a) and molar fractions of the non-bound vanadate (as the sum of the fractions of $HVO_4^{2-}/H_2VO_4^-/HV_2O_7^{3-}/$ $H_2V_2O_7^{2-}/V_4O_{12}^{4-}$; empty circles) and bound V(V) (filled circles) for PTSC (black symbols) and APTSC (gray symbols) from the integrated area of the ^{51}V NMR signals (b). {$c_{V(V)} = 1.0$ mM; V(V):L = 1:1; $T = 25.0$ °C, $I = 0.10$ M (KCl) in 30% (v/v) DMSO, 60% (v/v) H_2O, 10% (v/v) D_2O}.

2.4. Complex formation of STSC with vanadium(IV/V) ions and cytotoxicity studies

In order to investigate whether the solution stability of vanadium(IV/V) complexes of tridentate thiosemicarbazones and their cytotoxicity can be increased by exchange of the pyridyl nitrogen for a harder Lewis acid donor atom with higher affinity to the vanadium ions, STSC with a phenolate oxygen was chosen as a test compound (Chart 1).

The acid–base properties of STSC have already been studied in detail in our previous work [25], and the pK_a values determined here are in good agreement with the published data (Table 1). The pK_1 and pK_2 values of the ligand can be attributed to deprotonation of the phenolic OH group as well as the hydrazinic-NH of the thiosemicarbazide moiety. Noteworthy, the proton dissociation constant of the azomethine nitrogen atom (pK_2) of STSC is significantly higher compared to that of the α(N)-pyridyl TSCs. This can be explained by the different total charge of the ligands in the mono-protonated form: the α(N)-pyridyl TSCs are neutral, while STSC has one negative charge. It was found that STSC is mainly present in the neutral form (96% H_2L; 4% HL^-) at physiological pH and its log$D_{7.4}$ value [25] is considerably higher compared to those of the α(N)-pyridyl TSCs (Table 1).

The V(IV)O-binding ability of STSC was studied by pH-potentiometry and EPR methods. The pH-potentiometric data reveal the formation of mono-ligand species: $[V(IV)O(LH)]^+$, $[V(IV)O(L)]$ as well as $[V(IV)O(L)H_{-1}]^-$ comparably to previous data on complexes formed with other bivalent metal ions such as Cu(II) and Zn(II) [12]. Overall stability constants of the V(IV)O-STSC complexes are summarized in Table 1. Based on the deconvolution of the EPR spectra recorded at room temperature, a component spectrum (Fig. 6a) and isotropic EPR parameters (Table 2) of the complex $[V(IV)O(L)]$ could be calculated. Notably, data for $[V(IV)O(LH)]^+$ and $[V(IV)O(L)H_{-1}]^-$ could not be obtained with proper accuracy. This is most probably due to the low molar fraction of the protonated complex and the partial oxidation process in the pH range of the formation of $[V(IV)O(L)H_{-1}]^-$. Notably, the g_0 value of $[V(IV)O(L)]$ is slightly higher, although A_0 is in the same range, compared to the parameters of the corresponding complexes of Triapine, APTSC, and PTSC. It is noteworthy that the oxovanadium(IV) complex of salicylaldehyde semicarbazone (SSC) with (O^-,N,O^-) binding mode possesses significantly different EPR parameters ($g_0 = 1.9674$, $A_0 = 101.4$ G / 93.1×10^{-4} cm^{-1}) [37]. The most feasible binding mode in the $[V(IV)O(L)]$ complex of STSC is a coordination *via* the (O^-,N,S^-) donor set together with a deprotonated hydrazine moiety. This is in agreement with some X-ray crystal structures for ternary oxovanadium(IV) complexes of STSC or its derivatives formed with (N,N) bidentate aromatic co-ligands such as 1,10-phenanthroline or 2,2′-bipyridine in literature [23,38]. In the protonated $[V(IV)O(LH)]^+$ species the ligand most likely coordinates *via* (O^-,N,S) donor atoms (with protonated NH group), while $[V(IV)O(L)H_{-1}]^-$ is a mixed hydroxido complex ($=[V(IV)O(L)(OH)]^-$).

Due to the higher ligand basicity (higher pK_a values) of STSC compared to the α(N)-pyridyl TSCs, stronger ligand effectiveness is expected at higher pH values. Indeed, the increased oxovanadium(IV) binding ability of STSC over the α(N)-pyridyl TSCs is clearly reflected in the conditional stability constants (see logK' values calculated at pH 7.4 in Table 1) and the higher fractions of the bound metal ion in a broader pH range including pH 7.4 (*c.f.* Figs. 6b and 1). Thus, the involvement of the phenolate oxygen into the coordination instead of the pyridyl nitrogen results in more favorable complex formation with V(IV)O.

Since no redox reaction was observed, the V(V)–STSC system could be monitored over a wider pH range by ^{51}V NMR spectroscopy (Fig. 7a/b) compared to the α(N)-pyridyl TSCs. The recorded spectra represented formation of isomeric species (1) and (2) and three groups of signals were identified as follows: i) unbound V(V) as $HV(V)O_4^{2-}$ and $H_2V(V)O_4^-$; ii) bound V(V) as $[V(V)O_2(LH)]$ (1) and $[V(V)O_2(L)]^-$ (1) as well as iii) $[V(V)O_2(L)]^-$ (2) and $[V(V)O_2(L)H_{-1}]^{2-}$ (2) (Fig. 7b). Based on the pH-dependence of the chemical shifts of the peaks, equilibrium
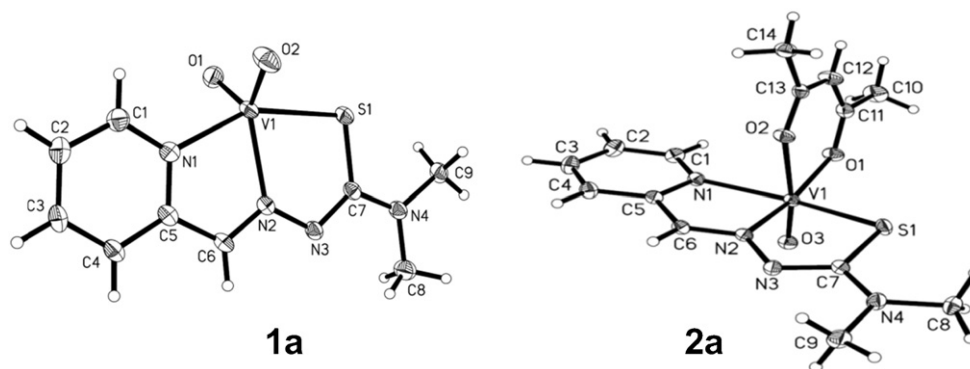
Table 4
Stability and protonation constants determined for the species formed in the V(V)O$_2$–TSC systems and their chemical shifts (δ (^{51}V)) {$T = 25.0$ °C, $I = 0.10$ M (KCl) in 30% (v/v) DMSO, 60% (v/v) H_2O, 10% (v/v) D_2O}.[a]

Ligand	Equilibrium	Constant
–	$HVO_4^{2-} + H^+ \rightleftharpoons H_2VO_4^-$ −561 ppm −536 ppm	log$K = 9.36(2)$
APTSC	$H_2VO_4^- + HL + H^+ \rightleftharpoons [VO_2(L)] + 2\,H_2O$ −416 ppm	log$K = 3.08(3)$
PTSC	$H_2VO_4^- + HL + H^+ \rightleftharpoons [VO_2(L)] + 2\,H_2O$ −421 ppm	log$K = 3.34(3)$
STSC	$[VO_2(L)]^- (1) + H^+ \rightleftharpoons [VO_2(LH)]$ −449 ppm −502 ppm	log$K = 3.56(1)$
STSC	$[VO_2(L)H_{-1}]^{2-} + H^+ \rightleftharpoons [VO_2(L)]^- (2)$ −539 ppm −577 ppm	log$K = 9.95(2)$
STSC	$H_2VO_4^- + H_2L \rightleftharpoons [VO_2(L)]^- (1) + 2\,H_2O$	log$K = 5.42(5)$
STSC	$H_2VO_4^- + H_2L \rightleftharpoons [VO_2(L)]^- (2) + 2\,H_2O$	log$K = 4.57(5)$

[a] Uncertainties (SD) of the last digits are shown in parentheses.

Fig. 5. ORTEP view of [V(V)O$_2$(L)] complex of PTSC (**1a**) and [V(IV)O(L)(acac)] complex of PTSC (**2a**) with thermal ellipsoids at 50% probability level. Selected bond distances and angles are summarized in Table 5.

constants were calculated for protonation of the HV(V)O$_4^{2-}$, [V(V)$_2$(L)]$^-$ (1) and [V(V)O$_2$(L)H$_{-1}$]$^{2-}$ (2) species (Table 4). For the major isomer [V(V)O$_2$(L)]$^-$ (1) formed between pH ~ 3 and ~11, our data suggest ligand coordination most probably *via* the (O$^-$,N^2,S$^-$) donor set together with protonation of the N^3 thiosemicarbazone nitrogen. This results in formation of [V(V)O$_2$(LH)] (1) with an (O$^-$,N^2,S)-binding mode, which is in agreement with literature reports on solid phase structures for [V(V)O$_2$(L)]$^-$ and [V(V)O$_2$(LH)] of STSC representing these coordination modes [22]. Based on the integrated areas the ratio of major and minor isomers of [V(V)O$_2$(L)]$^-$ is 6.4:1 and was detected at −449 ppm and −577 ppm, respectively. This significant difference between the two chemical shifts suggests that besides the tridentate (O$^-$,N^2,S$^-$)-binding mode also a rather different coordination mode exists. In the case of the analogous semicarbazone, SSC, a minor isomer was also found at a similar chemical shift (−575.5 ppm) [37]. In this minor species, the chalcogen atom seems to be non-coordinated and a (O$^-$,N^2,N^4)-binding mode is feasible. Notably, the [V(V)O$_2$(L)]$^-$ (2) isomer has no protonated form but is able to form a mixed hydroxide species [V(V)O$_2$(L)H$_{-1}$]$^{2-}$ (2) in the basic pH range.

Representative concentration distributions curves are shown for the V(V)–STSC system in Fig. 8 calculated with the aid of the determined

stability data (Table 4). It could be concluded that the species [V(V)O$_2$(L)]$^-$ (1) and (2) are predominant at neutral pH.

In order to compare the vanadium(IV/V) binding ability of the studied TSC ligands pM* values were also calculated at pH 7.4 (Table S2). pM* is the negative logarithm of the summed equilibrium concentration of the non-bound metal ion and its hydroxido species under the conditions employed. According to these values the ligand effectiveness is for both the V(IV)O and V(V) ions in the following order: Triapine < APTSC, PTSC ≪ STSC. Thus, the solution equilibrium studies clearly revealed that the exchange of the α-pyridyl nitrogen by a phenolate oxygen indeed resulted in the formation of complexes with distinctly higher stability. To investigate if this is also reflected in the biological activity, a cytotoxicity test of the system with highest stability (V(V) with STSC) was performed in analogy to the biological investigations of the α-pyridyl TSCs above. In these experiments, metal-free STSC showed hardly any activity with IC$_{50}$ value of >100 μM in all three cell lines (KB-3-1, SW480 and A2780 cells). In contrast, co-incubation of STSC with NaVO$_3$ in 1:1 ratio at pH 7.4 (with formation of [V(V)O$_2$(L)]$^-$) was found to increase the cytotoxicity especially in A2780 cells to an IC$_{50}$ of 27.4 ± 8.2 μM (in the other two cell lines the IC$_{50}$ value was still >100 μM). In general, it is well known that STSC possesses significantly lower antiproliferative activity [39] compared to the class of α(N)-pyridyl TSCs [7]. This can probably be explained by the fact that α(N)-pyridyl TSCs were found to be unambiguously more efficient chelators for Fe(II) than STSC over a wide pH range [25]. This indicates that in case of STSC the redox cycling of the intracellularly formed iron complexes, which is assumed to be crucial for the activity of thiosemicarbazones, is hampered [6].

3. Conclusions

In the presented study, stoichiometry and stability of vanadium(IV/V) complexes formed with Triapine and two derivatives with dimethylated terminal amino groups (APTSC and PTSC) were studied in 30% (w/w) DMSO/H$_2$O solvent mixture focusing on the most plausible species emerging at physiological pH. Stability constants

Table 5
Selected bond lengths, angles and torsions for **1a**, **2a** and PTSC.[a]

	1a	2a	PTSC[b]
V(IV)–O1 [Å]		1.984(1)	
V(IV)–O2 [Å]		2.155(1)	
V(IV)–O3 [Å]		1.608(1)	
V(V)–O1 [Å]	1.608(2)		
V(V)–O2 [Å]	1.617(2)		
V–S1 [Å]	2.3725(8)	2.4026(6)	
V–N1 [Å]	2.105(2)	2.150(1)	
V–N2 [Å]	2.149(2)	2.074(1)	
S1–C7 [Å]	1.737(3)	1.751(2)	1.686(1)
N2–N3 [Å]	1.355(3)	1.365(2)	1.359(1)
N2–C6 [Å]	1.291(3)	1.294(2)	1.294(1)
N3–C7 [Å]	1.325(3)	1.334(2)	1.373(1)
N4–C7 [Å]	1.328(4)	1.341(2)	1.342(1)
C5–C6 [Å]	1.439(4)	1.453(2)	1.466(2)
S–V–N2 [deg]	76.91(6)	79.08(4)	
N1–V–N2 [deg]	74.67(8)	77.42(5)	
S–V–N1 [deg]	151.38(7)	154.07(4)	
N2–V–O1 [deg]	121.2(1)	163.89(5)	
N2–V–O2 [deg]	129.1(1)		
N1–V–O1 [deg]	97.3(1)		
N1–V–O2 [deg]	97.4(1)		
O2–V–O3 [deg]		171.86(5)	
C6–N2–N3–C7 [deg]	−178.7(2)	−171.3(1)	177.6(1)
N2–N3–C7–S [deg]	−0.2(3)	4.0(2)	−4.9(1)

[a] Uncertainties (SD) of the last digits are shown in parentheses.
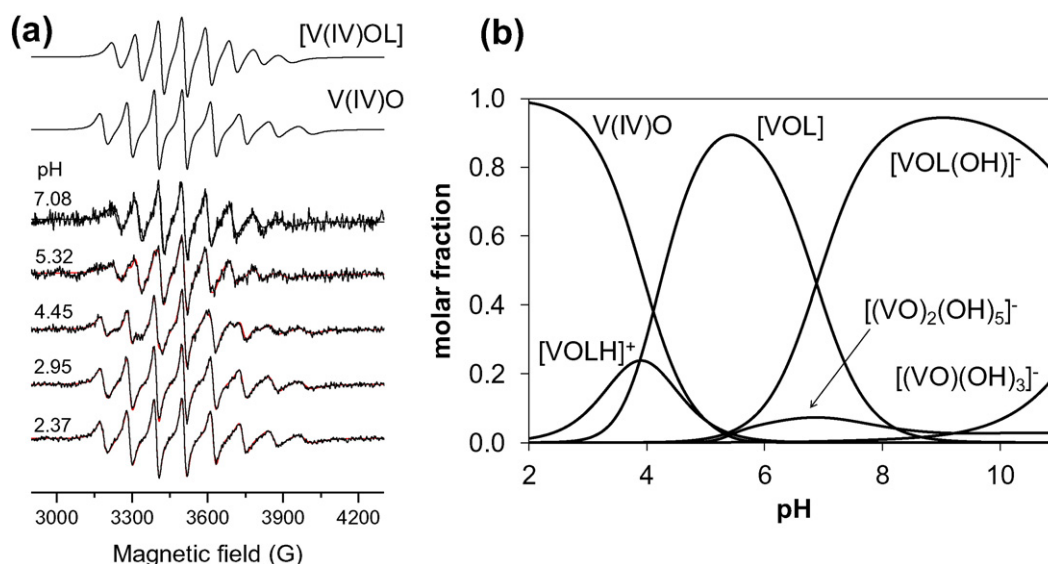[b] Taken from [7].

Table 6
In vitro cytotoxicity (IC$_{50}$ values in nM) of **1a**, **1b**, and **2a** in comparison to their metal-free ligands were measured in human cancer cell lines.

	KB-3-1	SW480	A2780
1a	67 ± 37	>500	3.3 ± 9
2a	60 ± 34	330 ± 4	2.5 ± 4
PTSC	92 ± 5	310 ± 13	2.5 ± 3
1b	1000 ± 7	700 ± 4	600 ± 17
APTSC	750 ± 30	400 ± 3	340 ± 6
Triapine	2800 ± 20[a]	400 ± 50[b]	N/A

[a] Taken from [36].
[b] Taken from [14].

Fig. 6. Experimental (black) and simulated (red) isotropic EPR spectra recorded for the V(IV)O–STSC system together with the calculated component EPR spectra of the various species with normalized spectral intensities for better comparison (a), and representative concentration distribution diagrams for V(IV)O complexes formed in the same system plotted against the pH calculated on the basis of the pH-potentiometric results (b) {c_{ligand} = 1.0 mM; V(IV)O:L = 1:1; T = 25.0 °C, I = 0.10 M (KCl) in 30% (w/w) DMSO/H$_2$O}.

and the most feasible coordination modes were determined by pH-potentiometry and EPR in the case of the oxovanadium(IV) complexes, while ^{51}V NMR spectroscopy was applied as the main tool for studying the complexation of vanadium(V). Formation of only mono-ligand oxovanadium(IV) complexes such as [V(IV)O(L)]$^+$ and [V(IV)O(L)(OH)] was found with Triapine, APTSC, and PTSC. Here, coordination of ligand most probably occurs in a tridentate mode via an (N$_{pyr}$,N,S$^-$) donor set, while the hydrazinic-N is deprotonated. Triapine was found to be an inefficient oxovanadium(IV) binder at neutral pH,

whereas the terminally dimethylation results in an enhancement of the complex stability. This is also true for V(V): Triapine was not able to bind V(V) at pH 7.4, whereas APTSC and PTSC form [V(V)O$_2$(L)] type complexes, which possessed even somewhat higher stabilities than the oxovanadium(IV) species.

Subsequently, vanadium complexes of PTSC and APTSC with adequate stability at physiological pH were synthesized and in detail characterized followed by cell culture tests in human cancer cell lines. Overall, the vanadium complexes exhibited widely identical anticancer
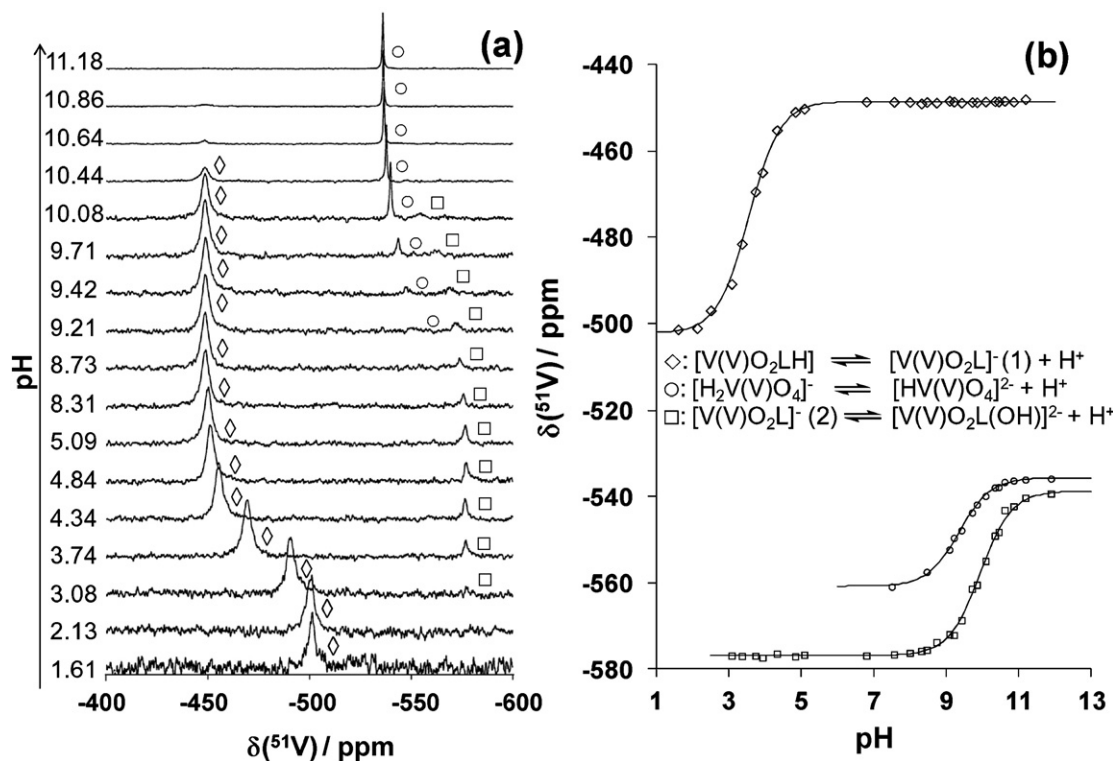
Fig. 7. ^{51}V NMR spectra recorded for the V(V)–STSC system at various pH values (a) and chemical shifts of the various groups of species plotted against the pH (b). ◇: [V(V)O$_2$LH] ⇌ [V(V)O$_2$L]$^-$ (1) + H$^+$; ○: [H$_2$V(V)O$_4$]$^-$ ⇌ [HV(V)O$_4$]$^{2-}$ + H$^+$; □: [V(V)O$_2$L]$^-$ (2) ⇌ [V(V)O$_2$L(OH)]$^{2-}$ + H$^+$. {$c_{V(V)}$ = 1.8 mM; V(V):L = 1:1.1; T = 25.0 °C, I = 0.10 M (KCl) in 30% (v/v) DMSO, 60% (v/v) H$_2$O, 10% (v/v) D$_2$O}.
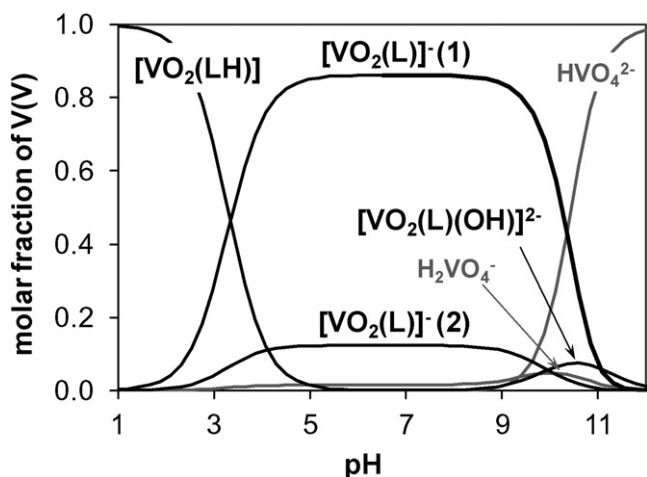
Fig. 8. Concentration distribution curves for the V(V)–STSC system. {$c_{V(V)}$ = 1.8 mM; V(V):L = 1:1.1; T = 25.0 °C, I = 0.10 M (KCl) in 30% (v/v) DMSO, 60% (v/v) H$_2$O, 10% (v/v) D$_2$O}.

activity as compared to the corresponding ligands implying that the vanadium binding in these complexes is not sufficient to impact on the biological activity.

In order to increase the solution stability of vanadium(IV/V)–TSC complexes, as a next step, STSC, a ligand containing a phenolate oxygen donor atom instead of the pyridyl nitrogen was investigated in our studies. The results showed that STSC forms complexes with oxovanadium(IV) characterized by an (O$^-$,N^2,S)-binding mode and a protonated hydrazinic NH moiety ([V(IV)O(LH)]$^+$). In addition, species with a completely deprotonated ligand coordinated through an (O$^-$,N^2,S$^-$) donor set ([V(IV)O(L)] and [V(IV)O(L)(OH)]$^-$) were observed (with V(V) similar species were detected). The stabilities of the vanadium(IV/V) complexes of STSC were found to be significantly higher than that of the α(N)-pyridyl TSCs. Cytotoxicity measurements of a STSC–V(V) complex revealed an increase of the anticancer activity compared to the very low activity of the metal-free STSC ligand. In general, the cytotoxic activity of STSC was strongly decreased compared to α(N)-pyridyl TSCs. Thus STSC derivatives with higher anticancer activity e.g. terminal dimethylated derivatives will be investigated in subsequent studies to further increase the stability and shift the biological activity to the low micromolar range.

4. Experimental

4.1. Chemicals

Triapine, PTSC, and APTSC were prepared as described previously [7, 31]. STSC was purchased from Sigma-Aldrich and used without further purification. The exact concentration of the ligand stock solutions together with the proton dissociation constants was determined by pH-potentiometric titrations with aid of the computer program HYPERQUAD [40]. NaVO$_3$, VOSO$_4$, KOH, D$_2$O, and DMSO-d_6 were purchased from Sigma-Aldrich and HCl, KCl as well as DMSO were from Reanal. The V(IV)O stock solution was prepared as described [41] and standardized for the metal ion concentration by permanganate titration. Vanadate stock solution was prepared by dissolving NaVO$_3$ in KOH solution and its concentration was calculated based on mass and total volume. Double distilled Milli-Q water was used for sample preparations.

All solvents used for synthesis were of analytical grade and used without further purification. V$_2$O$_4$(acac)$_2$ was synthesized according to literature procedures [32]. Elemental analyses were carried out on a Carlo Erba microanalyzer at the Microanalytical Laboratory of the University of Vienna. Electrospray ionization mass spectrometry (ESI-MS) was carried out with a Bruker Esquire 3000 instrument (Bruker

Daltonic, Bremen, Germany). Expected and experimental isotope distributions were compared. UV–vis spectra for the complexes were recorded on a Perkin Elmer Lambda 650 UV–vis spectrophotometer using samples dissolved in methanol (900–210 nm). ^{1}H and ^{13}C one- and two-dimensional NMR spectra were recorded in DMSO-d_6, with a Bruker Avance III 500 MHz FT-NMR spectrometer. The residual ^{1}H and ^{13}C present in DMSO-d_6 were used as internal references. ^{51}V NMR spectra for the complexes were recorded in DMSO-d_6 with a Bruker Avance DRX 500 MHz spectrometer. (Abbreviations for NMR data: py = pyridine, C$_{q, py}$ = quaternary carbon of pyridine.)

4.2. Synthesis of vanadium(IV/V) complexes of PTSC and APTSC

(2-Formylpyridine N,N-dimethylthiosemicarbazonato)dioxovanadium(V), [V(V)O$_2$(L)] complex of PTSC (**1a**): PTSC (115 mg, 0.55 mmol) was dissolved in hot methanol (5 mL), added to V$_2$O$_4$(acac)$_2$ (100 mg, 0.27 mmol) in methanol (5 mL) and the mixture was stirred for 3 min. The orange precipitate formed was filtered off, washed with cold methanol (−20 °C) and dried in vacuo. Yield: 118 mg (74%). Anal. Calcd. for C$_9$H$_{11}$N$_4$O$_2$SV (M_r = 290.22 g/mol): C, 37.25; H, 3.82; N, 19.31; S, 11.05. Found: C, 37.15; H, 3.68; N, 19.11; S, 11.20. ESI-MS in methanol (positive): m/z 313, [M + Na]$^+$; 329, [M + K]$^+$. UV–vis (methanol), λ$_{max}$, nm (ε, M^{-1} cm^{-1}): 221 (10,015), 281 (5615), and 490 (6940). ^{1}H NMR (500.10 MHz, DMSO-d_6): δ 8.58 (d, 1H, py, $^3J_{H,H}$ = 4 Hz), 8.54 (s, 1H, HC=N), 8.24 (m, 1H, py), 7.87 (d, 1H, py, $^3J_{H,H}$ = 8 Hz), 7.57 (m, 1H, py), and 3.27 (s, 6H, N(CH$_3$)$_2$). ^{13}C NMR (125.81 MHz, DMSO-d_6): δ 178.2 (C–S), 154.2 (C$_{q, py}$), 153.6 (C$_{py}$), 146.7 (HC=N), 143.5 (C$_{py}$), 125.7 (C$_{py}$), 125.4 (C$_{py}$), and 40.3 (N(CH$_3$)$_2$). ^{51}V NMR (500 MHz, DMSO-d_6): −427.5 ppm. After a few days crystals suitable for X-ray data collection were directly obtained from the mother liquor.

(3-Amino-2-formylpyridine N,N-dimethylthiosemicarbazonato)dioxovanadium(V), [V(V)O$_2$(L)] complex of APTSC (**1b**): APTSC (90 mg, 0.40 mmol) was suspended in methanol (4 mL), added to V$_2$O$_4$(acac)$_2$ (73 mg, 0.20 mmol) in methanol (4 mL) and the mixture was stirred for 1.5 h at room temperature. The dark-red precipitate formed was filtered off, washed with methanol and dried in vacuo. Yield: 77 mg (63%). Anal. Calcd. for C$_9$H$_{12}$N$_5$O$_2$SV (M_r = 305.23 g/mol): C, 35.41; H, 3.96; N, 22.94; S, 11.05. Found: C, 35.54; H, 3.80; N, 22.63; S, 10.59. ESI-MS in methanol (positive mode): m/z 329, [M + Na]$^+$; 344, [M + K]$^+$. UV–vis (methanol), λ$_{max}$, nm (ε, M^{-1} cm^{-1}): 257 (3030), 280 (2890), 299sh (2740), and 445 (3560). ^{1}H NMR (500.10 MHz, DMSO-d_6): δ 8.89 (s, 1H, HC=N), 7.83 (d, 1H, py, $^3J_{H,H}$ = 5 Hz), 7.36 (dd, 1H, py, $^3J_{H,H}$ = 9 Hz, $^4J_{H,H}$ = 1 Hz), 7.26 (dd, 1H, py, $^3J_{H,H}$ = 9 Hz, $^3J_{H,H}$ = 5 Hz), 6.64 (s, 2H, NH$_2$), and 3.22 (s, 6H, N(CH$_3$)$_2$). ^{13}C NMR (125.81 MHz, DMSO-d_6): δ 176.2 (C–S), 146.2 (HC=N), 145.7 (C$_{q, py}$), 142.5 (C$_{py}$), 135.5 (C$_{q, py}$), 128.5 (C$_{py}$), 126.9 (C$_{py}$), and 40.3 (N(CH$_3$)$_2$). ^{51}V NMR (500 MHz, DMSO-d_6): −430.0 ppm.

(Acetylacetonato(2-formylpyridine N,N-dimethylthiosemicarbazonato) oxovanadium(IV), [V(IV)O(L)(acac)] complex of PTSC (**2a**): under an argon atmosphere, PTSC (79 mg, 0.38 mmol) was added as a solid to a solution of VO(acac)$_2$ (100 mg, 0.38 mmol) in ethanol (10 mL) and the mixture was stirred for 1.5 h. The green precipitate formed was filtered off, washed with isopropanol, and dried in vacuo. Yield: 110 mg (78%). Anal. Calcd. for C$_{14}$H$_{18}$N$_4$O$_3$SV (M_r = 373.32 g/mol): C, 45.04; H, 4.86; N, 15.01; S, 8.59. Found: C, 44.86; H, 4.98; N, 14.72; S, 8.63. ESI-MS in methanol (positive mode): m/z 396, [M + Na]$^+$; 412, [M + K]$^+$. UV–vis (methanol), λ$_{max}$, nm (ε, M^{-1} cm^{-1}): 268 (10,740), 347sh (3955), and 433 (5930). Crystals suitable for X-ray data collection were obtained by slow diffusion of ether into a solution of **2a** in dichloromethane under an argon atmosphere.

4.3. Crystallographic structure determination of 1a and 2a

X-ray diffraction measurements were performed on a Bruker X8 APPEXII CCD diffractometer. A single crystal of suitable size was coated

with Paratone-N oil, mounted at room temperature on a cryo loop and cooled under a stream of cold N_2 maintained by a KRYOFLEX low-temperature apparatus. Crystals of **1a** and **2a** were positioned at 35 mm from the detector, and 1820/835 frames were measured, each for 30/60 s over 1° scan width. The data were processed using SAINT software [42]. The structures were solved by direct methods and refined by full-matrix least-squares techniques. Non-hydrogen atoms were refined with anisotropic displacement parameters. H atoms were placed at calculated positions and refined as riding atoms in the subsequent least squares model refinements. The following software programs and computer were used: structure solution, SHELXS-97 [43]; refinement, SHELXL-97 [43]; molecular diagrams, ORTEP [44]; computer: Intel CoreDuo. Crystal data and structure refinement details for **1a** and **2a** are given in Table S1. Crystallographic data have been deposited at the Cambridge Crystallographic Data Center with numbers CCDC1021658 and 1021659.

4.4. pH-potentiometric measurements

The pH-metric measurements for determination of the protonation constants of the ligands and the overall stability constants of the V(IV)O complexes were carried out at 25.0 ± 0.1 °C in DMSO:water 30:70 (w/w) as solvent and at an ionic strength of 0.10 M (KCl) in order to keep the activity coefficients constant. The titrations were performed with carbonate-free KOH solution of known concentration (0.10 M). The concentrations of the base and the HCl were determined by pH-potentiometric titrations. An Orion 710A pH-meter equipped with a Metrohm combined electrode (type 6.0234.100) and a Metrohm 665 Dosimat burette were used for the pH-metric measurements. The electrode system was calibrated to the pH $= -\log[H^+]$ scale in the DMSO/water solvent mixture by means of blank titrations (strong acid *vs.* strong base; HCl *vs.* KOH), similarly to the method suggested by Irving et al. [45] in pure aqueous solutions. The average water ionization constant, pK_w, is 14.52 ± 0.05 in DMSO:water 30:70 (w/w) at 25 °C, which corresponds well to the literature [8,9,46] and results in pH 7.26 as neutral pH. The reproducibility of the titration points included in the calculations was within 0.005 pH. The pH-metric titrations were performed in the pH range 2.0–12.6. The initial volume of the samples was 10.0 mL. The ligand concentration was 1 or 2 mM and metal ion to ligand ratios of 1:1–1:5 were used. The accepted fitting of the titration curves was always less than 0.01 mL. Samples were deoxygenated by bubbling purified argon through them for *ca.* 10 min prior to the measurements. In the case of $V^{IV}O$-containing samples, argon overpressure was used when metal ion solution was added to the samples in tightly closed vessels, which were prior completely deoxygenated by bubbling a stream of purified argon through them for *ca.* 20 min. Argon was also passed over the solutions during the titrations.

The protonation constants of the ligands were determined with the computer program HYPERQUAD [40], and PSEQUAD [47] was utilized to establish the stoichiometry of the complexes and to calculate the stability constants ($\log\beta$ ($M_pL_qH_r$)) using the literature data for V(IV)O hydroxido complexes [48]. It is noteworthy that hydrolysis constants of V(IV)O hydroxido complexes are not known in the literature for the applied solvent mixture. ($M_pL_qH_r$) is defined for the general equilibrium $pM + qL + rH \rightleftharpoons M_pL_qH_r$ as β ($M_pL_qH_r$) $= [M_pL_qH_r] / [M]^p[L]^q[H]^r$, where M denotes the metal ion (V(IV)O) and L the completely deprotonated ligands. In all calculations, exclusively titration data were used from experiments in which no precipitate was visible in the reaction mixture.

4.5. UV–vis spectrophotometric and ^{51}V NMR measurements

A Hewlett Packard 8452A diode array spectrophotometer was used to record the UV–vis spectra in the interval 260–820 nm. The path length was 1 cm. Protonation and stability constants and the individual spectra of the species were calculated by the computer program PSEQUAD [47]. The spectrophotometric titrations were performed on

samples of the pure TSCs or with V(IV)O; the concentration of ligand was 50 or 63 μM and the metal-to-ligand ratios were 1:1 and 1:2 over the pH range between 2 and 12.6 at an ionic strength of 0.10 M KCl in 30% (w/w) DMSO/H_2O at 25.0 ± 0.1 °C. For V(IV)O samples, spectra were recorded under anaerobic conditions.

^{51}V NMR studies were carried out on a Bruker Avance DRX500 instrument and a spectral window of 760 ppm, a 90° pulse angle and an acquisition time of 0.65 s with a relaxation delay of 0.5 s and a pulse width of 7 ms were used. V(V)OCl$_3$ was used as an external reference. The TSCs were dissolved in 30% (v/v) DMSO 60% H_2O and 10% D_2O at 25 °C in a concentration of 1.0 or 1.8 mM and the V(V)O$_2$-to-ligand ratios were 1:1 or 1:1.1. Samples contained 0.10 M KCl. Overall stability or stepwise constants for the complex formation equilibria were determined with the aid of the computer program PSEQUAD [47] on the basis of the integral values and chemical shifts using the literature data for the vanadates (H^+/V(V)) [49].

4.6. Determination of the distribution coefficient (D)

$D_{7.4}$ values of PTSC and APTSC were determined by the traditional shake flask method in *n*-octanol/buffered aqueous solution at 7.40 (HEPES, 0.01 M) at 25.0 ± 0.2 °C. Measurements and calculations were performed similarly as we described previously for Triapine and STSC [25].

4.7. EPR measurements and deconvolution of the spectra

All continuous-wave (CW) EPR spectra were recorded with a BRUKER EleXsys E500 spectrometer (microwave frequency 9.81 GHz, microwave power 10 MW, modulation amplitude 5 G, modulation frequency 100 kHz). EPR spectra were recorded at 1.0 mM of V(IV)O and the metal-to-ligand ratios were 1:1, 1:2, 1:2 and 1:4 for STSC, APTSC, PTSC, and Triapine, respectively, between pH ~ 2–8 in 30% (w/w) DMSO/H_2O mixture at an ionic strength of 0.10 M KCl. For the V(IV)O − Triapine, APTSC, PTSC and STSC systems 4, 4, 8 and 5 isotropic EPR spectra were recorded at room temperature. At higher pH the EPR signal disappeared possibly because of V(IV)O oxidation, although titrations were carried out under argon atmosphere. Oxidation could be excluded more efficiently in the case of PTSC and spectra of individual samples could be recorded up to pH 9.8.

At certain pH values, 0.10 mL of samples was taken out of the solutions into quartz EPR tubes and was measured individually in a Dewar containing liquid nitrogen (at 77 K). KOH solution was added to the stock solution to change the pH which was measured with an Orion 710A pH-meter equipped with a Metrohm combined electrode (type 6.0234.100).

Series of V(IV)O CW-EPR spectra recorded at 25 °C were simulated by the "two-dimensional" method using the 2D_EPR program [50]. The g_0, and A_0^V ($I = 7/2$) oxovanadium(IV) hyperfine coupling parameters were taken into account to describe each component curve. The relaxation parameters, α, β, and γ, defined the line widths through the equation $\sigma_{M_I} = \alpha + \beta M_I + \gamma M_I^2$, where M_I denotes the magnetic quantum number of the paramagnetic metal ions.

The anisotropic EPR spectra recorded at 77 K were analyzed individually with the EPR program [51]. For the V(IV)O complexes g_{ll}, $g_\perp$ axial g-tensor and A_{ll}^V, $A_\perp^V$ axial hyperfine tensor were taken into consideration. The following expressions are valid for the g values in the case of a d_{xy} ground state and an axial symmetry:

$$g_{II} = g_e - \frac{8\alpha^2\beta^2\xi}{\Delta E(x^2, y^2)} \text{ and } \quad g_\perp = g_e - \frac{2\beta^2\gamma^2\xi}{\Delta E(xz, y\,\dot{z})}.$$

Here, α, β, and γ are the vanadium $d_{x^2-y^2}^{22}$, d_{xy}, and $d_{xz,yz}$ orbital populations, ξ is the spin–orbit constant, $\Delta E(x^2 - y^2)$ and $\Delta E(xz,yz)$ are the

energy differences between the $d_{x^2-y^2}$, $d_{xz,yz}$ excited states, respectively, and the d_{xy} ground state.

For each spectrum, the noise-corrected regression parameter (R_j for the jth spectrum) was derived from the average square deviation (SQD) between experimental and calculated intensities. For the series of spectra, the fit is characterized by the overall regression coefficient R, calculated from the overall average SQD. The details of the statistical analysis were published previously [51]. The hyperfine and superhyperfine coupling constants and the relaxation parameters were obtained in field units (Gauss = 10^{-4} T) and were calculated to 10^{-4} cm^{-1} by the correspondence of A [10^{-4} cm^{-1}] ⇔ 0.4668643 g A [G].

4.8. Cell lines and culture conditions

The following human cell lines were used in this study: the colon carcinoma cell line SW480 (from American Type Culture Collection, Manassas, VA), the ovarian carcinoma cell line A2780 (from Sigma-Aldrich) and the epidermal carcinoma-derived cell line KB-3-1 (generously donated by D.W. Shen, Bethesda, USA). All cells were grown in RMPI 1640 supplemented with 10% fetal bovine serum (FCS), with the exception of SW480 cells with were cultivated in minimal essential medium with 10% FCS. Cultures were regularly checked for *Mycoplasma* contamination.

4.9. MTT assays

To determine cell viability, cells were plated (2×10^3 cells in 100 µL/well) in 96-well plates and allowed to recover for 24 h. Stock solutions (in DMSO) of the test compounds (APTSC, PTSC, STSC, **1a**, **2a**, **1b**) were diluted in complete culture medium and added to the plates (100 µL/well). The maximum DMSO content did not exceed 0.5%. Stock solution of the V(V)–STSC complex was prepared by addition of NaVO$_3$ in water to STSC in DMSO at a 1:1 metal-to-ligand ratio, followed by subsequent dilution with cell culture medium. After 72 h drug treatment, the proportion of viable cells was determined by the colorimetric MTT microculture assay following the manufacturer's recommendations (EZ4U, Biomedica, Vienna, Austria).

Abbreviations

1a	(2-formylpyridine N,N-dimethylthiosemicarbazonato) dioxovanadium(V)
1b	(3-amino-2-formylpyridine N,N-dimethylthiosemicarbazonato) dioxovanadium(V)
2a	(acetylacetonato(2-formylpyridine N,N-dimethylthiosemicarbazonato)oxovanadium(IV)
acac	acetylacetonate
APTSC	3-aminopyridine-2-carboxaldehyde N,N-dimethylthiosemicarbazone
CT	charge transfer
CW	continuous-wave
δ	chemical shift
$D_{7.4}$	distribution coefficient at pH 7.4
DMSO	dimethyl sulfoxide
Dp44mT	di-2-pyridylketone-4,4-dimethyl-3-thiosemicarbazone
ε	molar absorptivity
ESI-MS	electrospray ionization mass spectrometry
FCS	fetal bovine serum
HEPES	4-(2-hydroxyethyl)-1-piperazineethanesulfonic acid
MTT	3-(4,5-dimethyl-2-thiazolyl)-2,5-diphenyl-2H-tetrazolium bromide
PTSC	pyridine-2-carboxaldehyde N,N-dimethylthiosemicarbazone
SQD	average square deviation
SSC	salicylaldehyde semicarbazone
STSC	salicylaldehyde thiosemicarbazone
TSC	thiosemicarbazone
Triapine	3-aminopyridine-2-carboxaldehyde thiosemicarbazone
UV–vis	UV–visible

Appendix A. Supplementary data

Supplementary data to this article can be found online at http://dx.doi.org/10.1016/j.jinorgbio.2015.08.023.

References

[1] D.X. West, S.B. Padhye, P.B. Sonawane, Struct. Bond. (Berlin) 76 (1991) 1–50.
[2] J.R. Dilworth, R. Hueting, Inorg. Chim. Acta 389 (389) (2012) 3–15.
[3] J. Shao, B. Zhou, A.J. Di Bilio, L. Zhu, T. Wang, C.Q.J. Shih, Y. Yen, Mol. Cancer Ther. 5 (2006) 586–592.
[4] C.M. Nutting, C.M.L. van Herpen, A.B. Miah, S.A. Bhide, J.P. Machiels, J. Buter, C. Kelly, D. de Raucourt, K.J. Harrington, Ann. Oncol. 20 (2009) 1275–1279.
[5] T.B. Chaston, D.B. Lovejoy, R.N. Watts, D.R. Richardson, Clin. Cancer Res. 9 (2003) 402–414.
[6] Y. Ays, M.J.C. Long, J. Stubbe, J. Biol. Chem. 287 (2012) 35768–35778.
[7] C.R. Kowol, R. Trondl, P. Heffeter, V.B. Arion, M.A. Jakupec, A. Roller, M. Galanski, W. Berger, B.K. Keppler, J. Med. Chem. 52 (2009) 5032–5043.
[8] E.A. Enyedy, N.V. Nagy, E. Zsigo, C.R. Kowol, V.B. Arion, B.K. Keppler, T. Kiss, Eur. J. Inorg. Chem. (2010) 1717–1728.
[9] E.A. Enyedy, M.F. Primik, C.R. Kowol, V.B. Arion, T. Kiss, B.K. Keppler, Dalton Trans. 40 (2011) 5895–5905.
[10] Y. Yu, D.S. Kalinowski, Z. Kovacevic, A.R. Siafakas, P.J. Jansson, C. Stefani, D.B. Lovejoy, P.C. Sharpe, P.V. Bernhardt, D.R. Richardson, J. Med. Chem. 52 (2009) 5271–5294.
[11] M. Whitnall, J. Howard, P. Ponka, D.R. Richardson, Proc. Natl. Acad. Sci. U. S. A. 103 (2006) 14901–14906.
[12] P.J. Jansson, T. Yamagishi, A. Arvind, N. Seebacher, E. Gutierrez, A. Stacy, S. Maleki, D. Sharp, S. Sahni, D.R. Richardson, J. Biol. Chem. 290 (2015) 9588–9603.
[13] B.M. Paterson, P.S. Donnelly, Chem. Soc. Rev. 40 (2011) 3005–3018.
[14] C.R. Kowol, P. Heffeter, W. Miklos, L. Gille, R. Trondl, L. Cappellacci, W. Berger, B.K. Keppler, J. Biol. Inorg. Chem. 17 (2012) 409–423.
[15] D.X. West, A.E. Liberta, S.B. Padhye, R.C. Chikate, P.B. Sonawane, A.S. Kumbhar, R.G. Yerande, Coord. Chem. Rev. 123 (1993) 49–71.
[16] J. Shao, W.G. Bao, H. Tian, B. Li, X.F. Zhao, X. Qiao, J.Y. Xu, Dalton Trans. 43 (2014) 1663–1671.
[17] H. Beraldo, D. Gambino, Mini Rev. Med. Chem. 4 (2004) 31–39.
[18] T.S. Lobana, R. Sharma, G. Bawa, S. Khanna, Coord. Chem. Rev. 253 (2009) 977–1055.
[19] S.A. Elsayed, A.M. El-Hendawy, S.I. Mostafa, B.J. Jean-Claude, M. Todorova, I.S. Butler, Bioinorg. Chem. Appl. (2010), Article number: 149149 http://dx.doi.org/10.1155/2010/149149.
[20] N.A. Lewis, F. Liu, L. Seymour, A. Magnusen, T.R. Erves, J. Faye Arca, F.A. Beckford, R. Venkatraman, A. González-Sarrías, F.R. Fronczek, D.G. VanDerveer, N.P. Seeram, A. Liu, W.L. Jarrett, A.A. Holder, Eur. J. Inorg. Chem. (2012) 664–677.
[21] I.C. Mendes, L.M. Botion, A.V.M. Ferreira, E.E. Castellano, H. Beraldo, Inorg. Chim. Acta 362 (2009) 414–420.
[22] L.S. Vojinovic-Jesic, V.M. Leovac, M.M. Lalovic, V.I. Cesljevic, L.S. Jovanovic, M.V. Rodic, V. Divjakovic, J. Serb. Chem. Soc. 76 (2011) 865–877.
[23] M. Sutradhar, T.R. Barman, G. Mukherjee, M.G.B. Drew, S. Ghosh, Inorg. Chim. Acta 363 (2010) 3376–3383.
[24] P.I. da S. Maia, F.R. Pavan, C.Q.F. Leite, S.S. Lemos, G.F. de Sousa, A.A. Batista, O.R. Nascimento, J. Ellena, E.E. Castellano, E. Niquet, Polyhedron 28 (2009) 398–406.
[25] É.A. Enyedy, É. Zsigó, N.V. Nagy, C.R. Kowol, A. Roller, B.K. Keppler, T. Kiss, Eur. J. Inorg. Chem. (2012) 4036–4047.
[26] D. Wang, M. Ebel, C. Schulzke, C. Grüning, S.K.S. Hazari, D. Rehder, Eur. J. Inorg. Chem. (2001) 935–942.
[27] T.S. Smith, R. LoBrutto, V.L. Pecoraro, Coord. Chem. Rev. 228 (2002) 1–18.
[28] N.D. Chasteen, in: L.J. Berliner, J. Reuben (Eds.), Biological Magnetic Resonance, vol. 3, Plenum Press, New York 1981, pp. 53–119.
[29] S. Gorelsky, G. Micera, E. Garribba, Chem. Eur. J. 16 (2010) 8167–8180.
[30] J. García-Tojal, B. Donnadieu, J.P. Costes, J.L. Serra, L. Lezama, T. Rojo, Inorg. Chim. Acta 333 (2002) 132–137.
[31] R. McElhinney, J. Chem. Soc. C (1966) 950–955.
[32] K. Oyaizu, E.L. Dewi, E. Tsuchida, J. Electroanal. Chem. 498 (2001) 136–141.
[33] M. Pessôa, G.F.S. Andrade, V.R. Paoli Monteiro, M.L.A. Temperini, Polyhedron 20 (2001) 3133–3141.
[34] A.W. Addison, T.N. Rao, J. Reedijk, J. van Rijn, G.C. Verschoor, J. Chem. Soc. Dalton Trans. (1984) 1349–1356.
[35] B. Koo, Y. Jang, U. Lee, Bull. Korean Chem. Soc. 24 (2003) 1014–1016.

[36] P. Heffeter, C. Pirker, C.R. Kowol, G. Herrman, R. Dornetshuber, W. Miklos, U. Jungwirth, G. Koellensperger, B.K. Keppler, W. Berger, Biochem. Pharmacol. 83 (2012) 1623–1633.
[37] E.A. Enyedy, G.M. Bognar, N.V. Nagy, T. Jakusch, T. Kiss, D. Gambino, Polyhedron 67 (2014) 242–252.
[38] J. Lu, H. Guo, X. Zeng, Y. Zhang, P. Zhao, J. Jiang, L. Zang, J. Inorg. Biochem. 112 (2012) 39–48.
[39] P. Ying, P. Zeng, J. Lu, H. Chen, X. Liao, N. Yang, Chem. Biol. Drug Des. (2015), http://dx.doi.org/10.1111/cbdd.12535.
[40] P. Gans, A. Sabatini, A. Vacca, Talanta 43 (1996) 1739–1753.
[41] I. Nagypal, I. Fabian, Inorg. Chim. Acta 61 (1982) 109–113.
[42] SAINT-Plus, Version 7.68a and APEX2, Bruker-Nonius AXS Inc., Madison, WI, USA, 2008.
[43] G.M. Sheldrick, Acta Crystallogr. A64 (2008) 112–122.
[44] M.N. Burnett, G.K. Johnson, ORTEP III, Report ORNL-6895, Oak Ridge National Laboratory, Oak Ridge, TN, 1996.
[45] H.M. Irving, M.G. Miles, L.D. Pettit, Anal. Chim. Acta 38 (1967) 475–488.
[46] SCQuery, The IUPAC Stability Constants Database, Academic Software (Version 5.5), Royal Society of Chemistry, 1993–2005.
[47] L. Zékány, I. Nagypál, in: D.L. Leggett (Ed.), Computational Methods for the Determination of Stability Constants, Plenum Press, New York 1985, pp. 291–353.
[48] E. Kiss, K. Kawabe, A. Tamura, T. Jakusch, H. Sakurai, T. Kiss, J. Inorg. Biochem. 95 (2003) 69–76.
[49] K. Elvingson, A. González Baró, L. Pettersson, Inorg. Chem. 35 (1996) 3388–3393.
[50] A. Rockenbauer, T. Szabó-Plánka, Zs. Árkosi, L. Korecz, J. Am. Chem. Soc. 123 (2001) 7646–7654.
[51] A. Rockenbauer, L. Korecz, Appl. Magn. Reson. 10 (1996) 29–43.